INTERNATIONAL JOURNAL OF CONSERVATION SCIENCE
ISSN: 2067-533X Volume 17, Issue 3, 2026: 1147-1158 www.ijcs.ro
DOI: 10. 36868/IJCS.2026.03.19

APPLICATION OF CONSUMER MOBILE DEVICES FOR LANDFORM MAPPING: A CASE STUDY OF THE MOUND AT WAWEL, KRAKÓW

Roksana ZARYCHTA[1,*]

[1] Institute of Law, Economics and Administration, University of the National Education Commission, Krakow, Podchorążych 2, 30-084 Kraków, Poland

Abstract

3D reconstruction of sites and objects using devices equipped with LiDAR scanners is becoming increasingly popular. However, the costs associated with purchasing such equipment remain very high. For this reason, consumer mobile devices such as the iPhone, into which Apple Inc. has been integrating LiDAR sensors since 2020, are worth considering. This article presents the use of the iPhone 15 Pro to scan a small mound located in the outer courtyard of Wawel Royal Castle in Kraków. The experiment demonstrated that the iPhone 15 Pro performs very well when scanning this type of feature, and the resulting point cloud, after further processing, yields very promising results in the form of a Digital Elevation Model (DEM).

Keywords: *iPhone; LiDAR; SfM; DEM; mound; Wawel; Kraków*

Introduction

The use of devices equipped with LiDAR (Light Detection and Ranging) scanners is gaining popularity due to the rapid acquisition of large volumes of data and their high accuracy. This results from the capability of LiDAR technology to measure distances by emitting laser light that reaches the surface of an object. Based on differences in the return time of the laser pulse, signal strength, frequency shift, and other parameters, it is possible to reconstruct the three-dimensional geometry of the scanned object [1]. LiDAR data, typically in the form of a point cloud, are characterized by high spatial accuracy and density and can be collected from airborne and terrestrial platforms, both stationary and mobile [2].

In Poland, the most commonly used source of LiDAR data comprises products derived from ALS (Airborne Laser Scanning), namely the Digital Elevation Model (DEM) and the Digital Surface Model (DSM), which are publicly available via the National Geoportal (https://www.geoportal.gov.pl). These data are provided in various horizontal and vertical (i.e., elevation) coordinate systems and cover different time periods and spatial resolutions. The use of such data is an excellent solution when analyzing terrain or objects covering large areas. However, difficulties arise in the case of small-scale studies, as the highest available resolution offered by the National Geoportal (point cloud: 4 – 20 pts/m²; DEM: 1 – 5 m; DSM: 0.5 – 1 m) is insufficient.

To achieve a high-resolution point cloud of the studied object, Terrestrial Laser Scanners (TLS) or mobile laser scanners employing Simultaneous Localization and Mapping (SLAM) technology may be utilized; however, the costs associated with their acquisition remain considerable. A viable alternative is the use of terrestrial photogrammetry, specifically the

* Corresponding author: roksana.zarychta@uken.krakow.pl

Structure from Motion (SfM) method, which enables three-dimensional reconstruction of the object based on two-dimensional images captured from varying distances and angles [3], [4]. Numerous studies to date have documented the application of SfM for purposes such as identifying geological structures and studying outcrops [5], modelling the topography of shallow braided rivers [6], monitoring coastal dunes [7], digitizing historical documents [8], and analyzing changes in glacier surface elevation [9]. To enhance reconstruction accuracy, SfM can be integrated with LiDAR technology, which has been incorporated into popular consumer mobile devices such as the iPhone and iPad. Since 2020, Apple Inc. has implemented LiDAR scanners in these devices primarily to support augmented reality (AR) applications and to improve photo and video quality in low-light conditions [10]. Notably, iPhones have garnered significant consumer interest. LiDAR technology has been available in these devices since the 12th generation, specifically in the Pro and Pro Max models.

The application of iPhones equipped with built-in LiDAR scanners is relatively broad. Various studies to date have explored their use for measuring and mapping trees [11], capturing 3D forensic data at crime and crash scenes [12], engineering applications [13], inspection and measurement in the mineshaft sinking process [14], inventorying surface defects on building walls [15], low-cost 3D building documentation [16], assessing damage to forest road wearing courses [17], documenting cultural heritage [18], and applications in the geosciences [19].

Accordingly, an experiment was undertaken using an iPhone 15 Pro equipped with a built-in LiDAR scanner to map one of the archaeological features located in Kraków. The aim of the study was to reconstruct a small mound situated on Wawel Hill and present it in the form of a visualization that includes both its hypsometry and shaded relief.

Experimental part

Object of the study

The study object selected was a landform located in Kraków, on Wawel Hill. Its position is defined by the following geographic coordinates: 50°03'13.43"N, 19°56'04.41"E (Fig. 1).

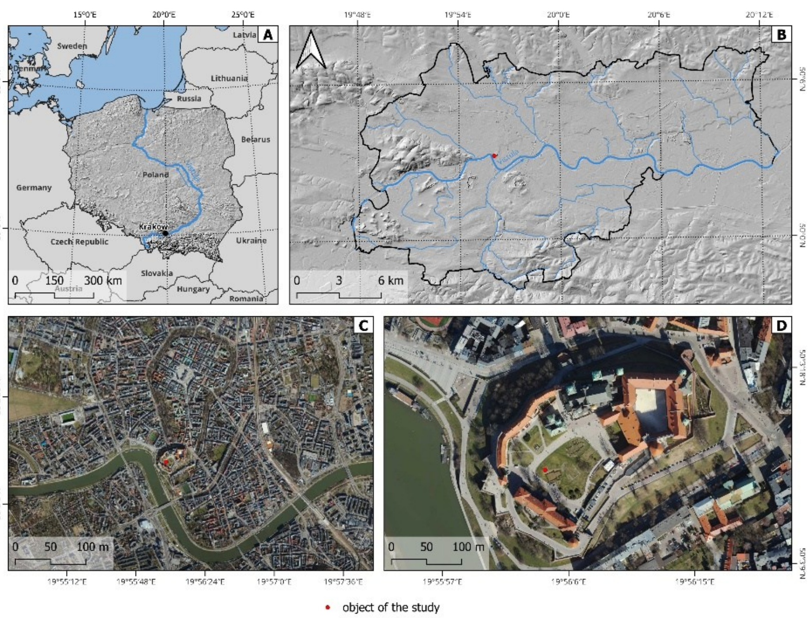

Fig. 1. Location of Kraków within Poland and Central Europe (A); the study object within Kraków (B), the Old Town (C), and Wawel Hill (D) [20], [21]

The analyzed feature is located in the outer courtyard of the Wawel Royal Castle, opposite the Thieves' Tower, in close proximity to the remains of St. George's Church. It has the shape of an almost regular cone, resembling a mound (Fig. 2). It is a classic archaeological witness, preserving the last fragment of a complete sequence of cultural layers (after the ground level was lowered between 1957 and 1960), accumulated from the Paleolithic period until 1960. It is most likely a replica of an earthen mound that stood in the same location (beneath the current road) until the 18th/19th century [22]. This mound was selected as the subject of the present experiment due to its small area, height, and, most importantly, its shape.

Fig. 2. Location of the study object in the Outer Courtyard of the Wawel Royal Castle

Materials and methods

The study was conducted using a popular consumer mobile device manufactured by Apple Inc., namely the iPhone 15 Pro 128 GB, which is equipped with a triple-lens camera system with the following specifications:

- main lens: 48MP, 24 mm, ƒ/1.78 aperture, second-generation sensor-shift optical image stabilization, 100% Focus Pixels, support for super-high-resolution photos,
- ultra-wide lens: 12MP, 13 mm, ƒ/2.2 aperture, 120° field of view, 100% Focus Pix-els,
- telephoto lens: 12MP 2x, 48 mm, ƒ/1.78 aperture, second-generation sensor-shift optical image stabilization, 100% Focus Pixels; 12MP 3x, 77 mm, ƒ/2.8 aperture, optical image stabilization [23] (Fig. 3).

Fig. 3. iPhone 15 Pro with built-in LiDAR scanner (red frame), flash (green frame), and rear cameras (1 – telephoto lens, 2 – ultra-wide-angle lens, 3 – main lens)

The device is additionally equipped with a LiDAR scanner, located near the camera lenses and appearing as a black dot approximately 6 mm in diameter (Fig. 3). Although Apple Inc. does not provide detailed information on the technical specifications of the LiDAR in this smartphone model, it has been determined that it is a Time-of-Flight (ToF) sensor, namely the Sony IMX591 LiDAR SPAD, with a resolution of 0.01 megapixels and a pixel pitch of 10.1 micrometers [24].

The experiment was conducted in two stages. The first involved fieldwork, while the second focused on analytical tasks. The fieldwork consisted of conducting field measurements of the studied mound, creating its photographic documentation, and carrying out archival research at the Wawel Royal Castle Archive. The analytical stage focused on processing the acquired data and generating visualizations. A concise overview of each stage of the work carried out is presented in Figure 4.

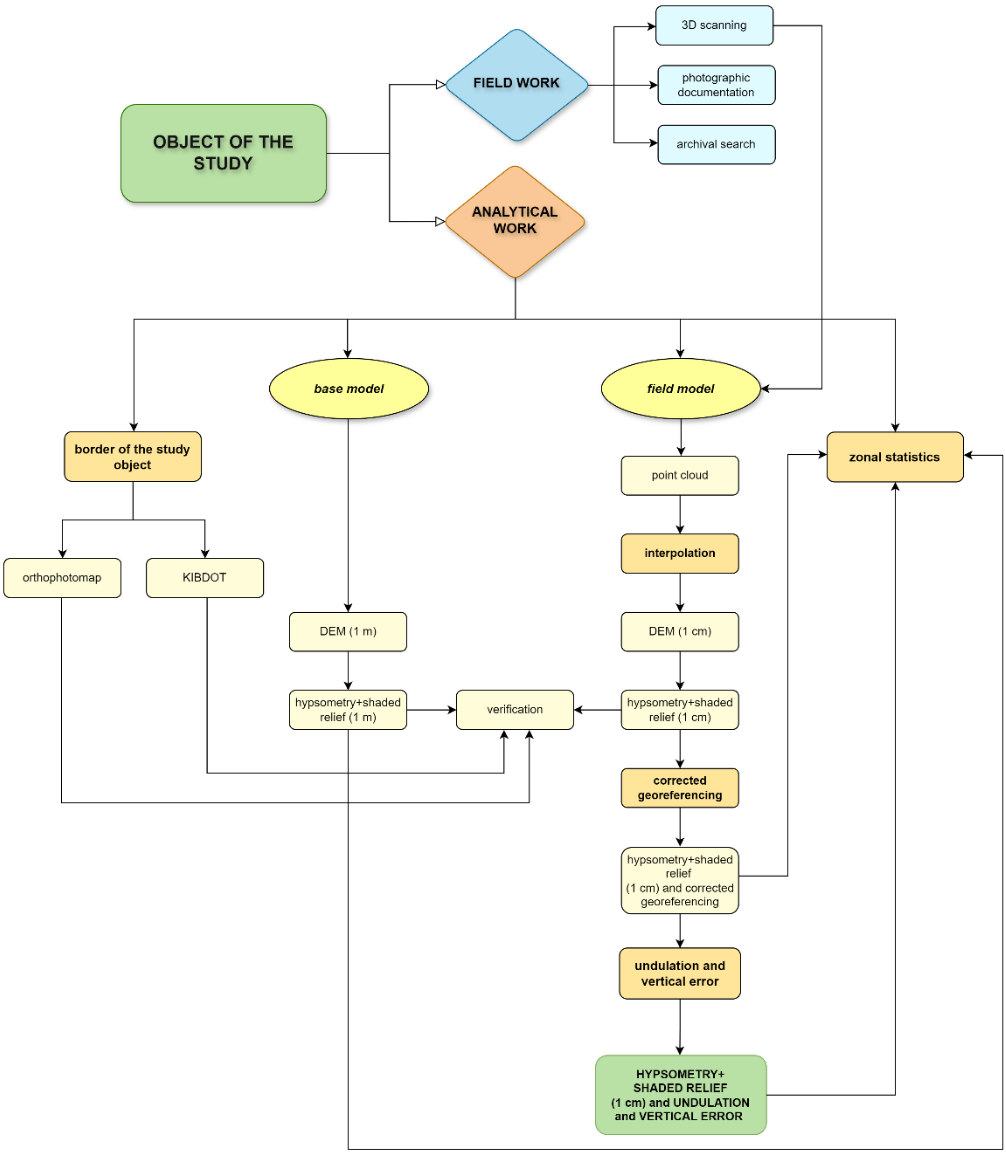

Fig. 4. Diagram of the experiment workflow

Results and discussion

Field work

Field measurements (referred to in the article as "scanning") were conducted on July 10, 2024, at 7:45 AM under very good weather conditions (i.e., clear skies and full sunlight) using the PIX4Dcatch 2.0.1 (Pix4D SA, Switzerland) application. Before starting the measurements, parameters were taken into account, which are presented in Table 1. At the time of measurement, the GPS in the application indicated a horizontal accuracy of approximately 4.73 m and a vertical accuracy of 3.39 m.

Table 1. Parameters from PIX4Dcatch 2.0.1

Type	Parameter	Value
Image Overlap	Overlap	90%
Device Pose	Distance	1 cm
	Angle	20°

The scanning process began on the northern side of the studied form, moving in a circular motion counterclockwise while holding the device at a constant angle. Data were collected in the WGS84 coordinate system. The completion of each circuit coincided with ascending to a higher part of the object (up to its summit) (Fig. 5).

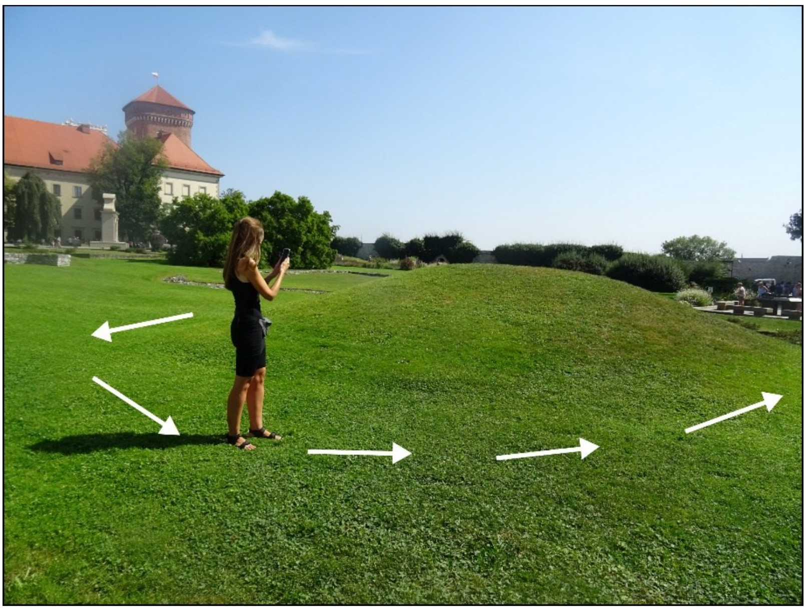

Fig. 5. View of the studied object with the scanning direction

The scanning was conducted in several measurement cycles, each lasting approximately 6 minutes. During the scanning, the 3D model generated from the recorded video frames with assigned geolocation data was continuously monitored and analyzed in the application. This allowed for ongoing assessment of the coverage level of the studied object's surface with data. Ultimately, the cycle that provided a full and complete representation of the shape and surface of the examined mound was selected for further analysis (Fig. 6).

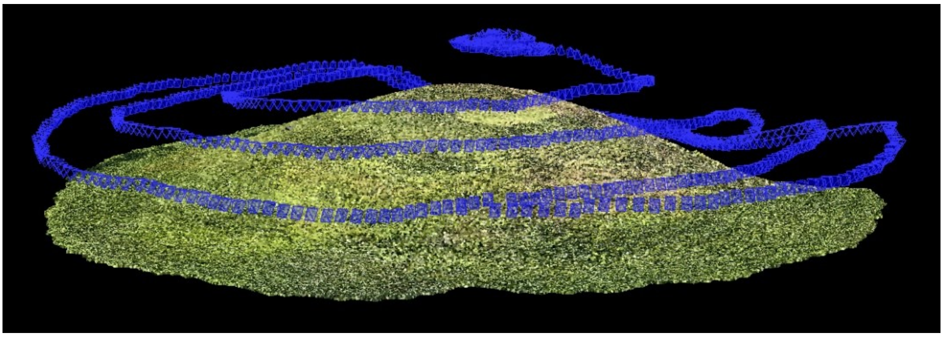

Fig. 6. View from the PIX4Dcatch 2.0.1 app of the studied object, showing the final scanning result (blue line – scanning path)

Analytical work

The analytical work included a series of tasks related to data processing, analysis, and the generation of visualizations based on both the base model and the terrain model. Additionally, the boundary of the studied object was determined based on the orthophotomap [21] and the National Integration of Topographic Object Databases (KIBDOT) [25] (Fig. 7).

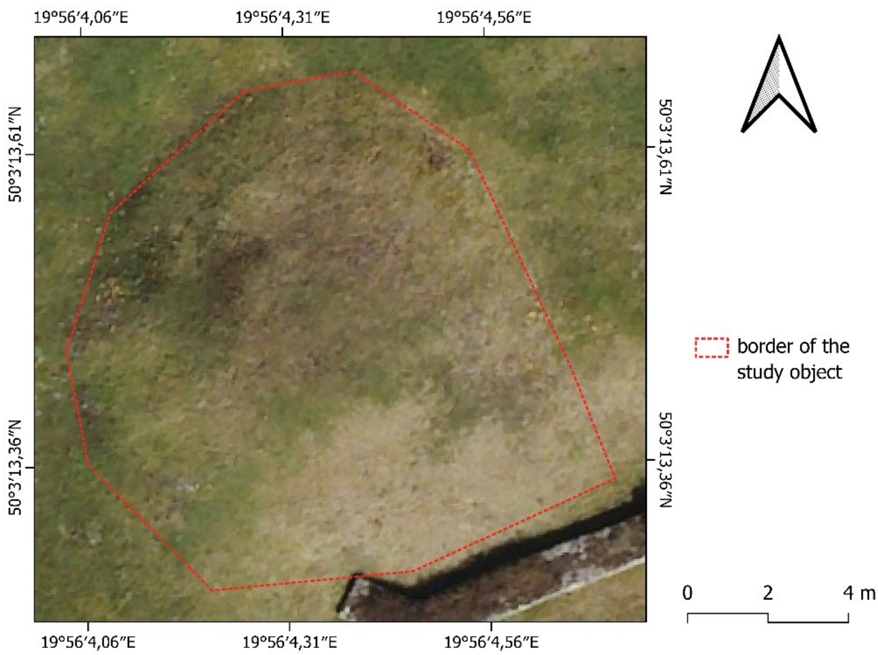

Fig. 7. Studied object on the orthophotomap

Base model

A Digital Elevation Model (DEM) was used, obtained from the National Geoportal (https://www.geoportal.gov.pl), with sheet ID M-34-64-D-d-1-4, in the horizontal coordinate system PL-1992—EPSG: 2180 and the vertical system PL-EVRF2007-NH, featuring a spatial resolution of 1.00 m, a mean vertical error of 0.10 m, and a mean positional error of 0.25 m (current as of 2023-09-08). Based on the DEM, a base model was generated, including hypsometry and hillshading (Fig. 8), which due to its low resolution (1 m) was used solely for comparison with the final terrain model created using iPhone scanning.

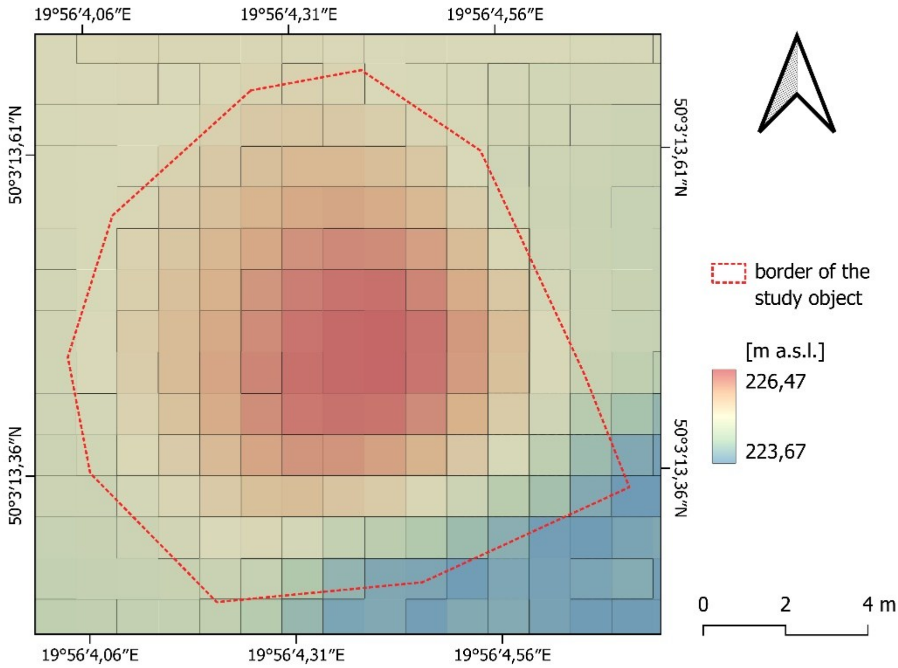

Fig. 8. Base model of the studied object

Terrain model

The data acquired during the field scanning was uploaded to the cloud for photogrammetric processing on PIX4D servers, where they were made available in PIX4Dcloud (https://cloud.pix4d.com). As a result, the 3D reconstruction of the studied mound was based on 819 RGB images, each accompanied by a corresponding depth file and confidence file (Table 2). Particularly important were the depth files derived from the LiDAR sensor, which enhanced the quality of the captured data (RGB images), as they contained information on the distance between the device and the analyzed object.

Table 2. Summary of the photogrammetry process

Name	Description
Image Input	819 images, 819 depth files, 819 confidence files
Dataset	819 out of 819 images were calibrated (100.0%)
Camera Optimization	0.44% relative difference between initial and optimized parameters
Median Number of Matches per Camera	3187
Average Ground Sampling Distance (GSD)	0.002035 m
Cameras Calibrated	819
Cameras Geolocated	819

As a result of the reconstruction, a set of geospatial output files was obtained and made available in PIX4Dcloud as a DSM (Digital Surface Model), Orthomosaic, 3D Textured Mesh, and Point Cloud in the WGS84 / UTM zone 34N coordinate system – EPSG: 32634. These were characterized by a very good Ground Sample Distance (GSD) of 0.002035 m (Fig. 9, Table 2).

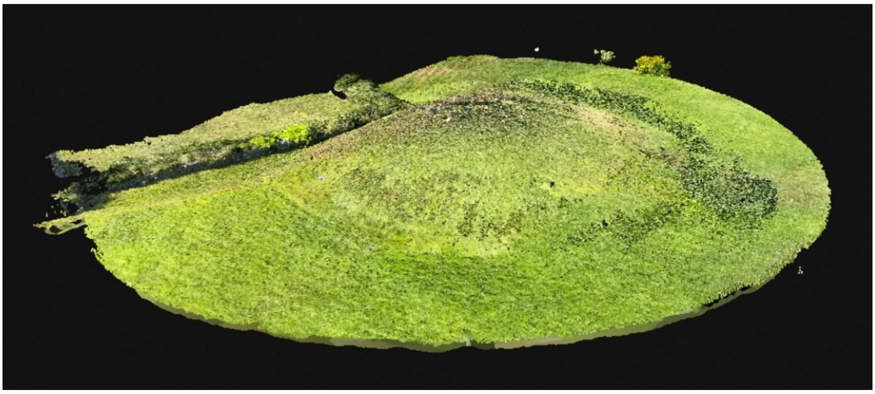

Fig. 9. Point cloud with applied texture presenting the studied object, generated in PIX4Dcloud

The point cloud representing the studied object was downloaded from PIX4Dcloud; it consisted of 17,390,141 points and featured low geolocation errors (Table 3). In summary, the obtained results indicate very good vertical and horizontal accuracy of the point cloud, which is why it was used for further geometric operations and spatial analyses in this experiment.

Table 3. Geolocation errors of the point cloud

	Error X	Error Y	Error Z
Mean [m]	0.009195	0.006761	0.001058
Sigma [m]	0.075641	0.052228	0.017795
RMS Error [m]	0.076198	0.052663	0.017826

Next, the point cloud was imported into CloudCompare v2.13.2 (CloudCompare v2.13.2, 2024; http://www.cloudcompare.org/), where the spatial distribution of points was verified from various perspectives. Since the computed point cloud contained outliers (i.e., noise), an attempt was made to remove them. To this end, the Statistical Outlier Removal (SOR) filter was applied. This tool first calculates the average distance from each point to its neighbors and then removes those that lie farther than the average distance increased by a multiple of the standard deviation. In this case, the best results were obtained using 30 points to estimate the mean distance (parameter 1: number of points to use for mean distance estimation) and a standard deviation multiplier threshold of 5 (parameter 2: standard deviation multiplier threshold – nSigma). As a result, 183,960 points were removed, leaving a filtered point cloud consisting of 17,206,181 points.

The filtered point cloud was imported into Surfer 27 software (Surfer; Golden Software; Golden, CO, USA, 2023), where it underwent an interpolation procedure. Due to the very large number of points forming the cloud, a decision was made to use one of the popular deterministic methods, namely the Inverse Distance Weighting (IDW) method. This method allows for the rapid estimation of a value at a location where no measurement was taken, based on the weighted average of values from points located near the interpolated location [26]. The interpolated value is calculated using the following formula [27]:

$$Z^*_{IDW}(x) = \frac{\sum_{i=1}^{n} w_i z_i}{\sum_{i=1}^{n} w_i}, w_i = \frac{1}{d_i^p},$$

where: z_i – the value of the variable at point i; w_i – the weight assigned to point i, inversely proportional to the distance d_i from point x; p – the power coefficient that controls how quickly the influence of distant points decreases.

In the analyzed case, default values were used for the parameters Weighting Power (2) and Smoothing Factor (0), as the dataset contained a very large number of points, and changing these values had no noticeable effect, either statistically or visually.

After the interpolation procedure was completed, the data were imported into QGIS 3.32.3 (QGIS Geographic Information System. QGIS Association, 2023, http://www.qgis.org/), where a terrain model was generated, incorporating hypsometry and hillshading. This model was compared with the orthophotomap, KIBDOT, and the base model. As a result, a slight northward displacement of the generated terrain model relative to the boundary of the analyzed feature was observed. This was due to horizontal error originating from GPS measurements (i.e., 4.73 m). Therefore, a correction of the current georeferencing of the terrain model was carried out. The most effective transformation type during the raster georeferencing adjustment proved to be the first-order polynomial (affine transformation), as it did not cause significant deformation and aligned the model extent very well with the boundary of the feature. It is worth noting that in the applied transformation method, point fitting involves translation, rotation, and scaling [28]. As a result, the mean error (horizontal error) of the corrected geolocation was 0.6 m, which is 4.13 m less than the horizontal error from the GPS measurements.

In the next step, elevation values across different parts of the studied landform were analyzed in both the base model and the terrain model to assess their differences. The terrain model displayed significantly higher elevation values than the base model, as the iPhone's GPS did not take into account the geoid height relative to the WGS84 ellipsoid. This resulted from the coordinate system used during the scanning process. Therefore, geoid undulation (i.e., the difference in elevation between the geoid and the ellipsoid) was calculated for the terrain model [27]. The undulation is defined by the following formula [29]:

$$N = H_E - H_O,$$

where: N – the geoid height; H_E – the GPS height above the reference ellipsoid; H_O – the orthometric height (the height over the defined geoid determined through Earth gravitation and mean sea level).

In the analyzed case, the geoid undulation amounted to 39.67 m for the quasi-geoid model PL-geoid2021 [30].

Subsequently, the raster calculator in QGIS 3.32.3 was used to reduce the existing elevation values of the terrain model by the calculated geoid undulation value, thus obtaining orthometric height values for the entire terrain model. In addition, the vertical GPS error (3.39 m) was added to the results in order to obtain elevation values as close as possible to those from the base model. Ultimately, the elevation values obtained from the terrain model differed only slightly from those recorded in the base model, with an average difference of 0.72 m (Table 4).

Table 4. Selected zonal statistics of the base model (BM) and the terrain model (TM) (including only the area within the boundaries of the studied landform)

Model type		Statistics Min [m]	Max [m]	Mean [m]
Base model (BM)		223.67	226.47	225.43
Terrain model (TM)	without geoid height (TM_A)	259.25	262.08	260.99
	reduced by the geoid height and increased by 3.39 m (TM_B)	222.97	225.80	224.71
	TM_A - BM	35.58	35.61	35.56
	BM- TM_B	0.7	0.67	0.72

Ultimately, a terrain model was obtained in the form of a visualization, comprising hypsometry along with shaded relief, which is characterized by very good spatial resolution (1 cm) (Fig. 10) compared to the base model, as well as very low horizontal errors and relatively low vertical errors. Figure 10 clearly outlines the extent of the studied feature, with its summit area also visible. Although the terrain beyond the boundary of the studied feature is accurately represented, the presence of artifacts should be taken into account. These artifacts result solely from the fact that during scanning of the lower part of the analyzed form, data from the neighboring terrain were also captured and included in the interpolation procedure.

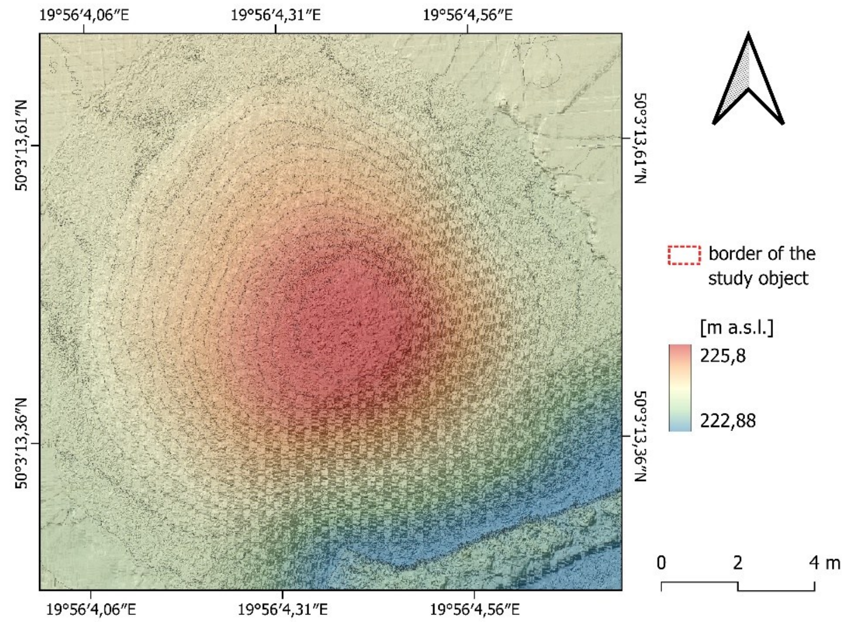

Fig. 10. Terrain model of the studied object

Conclusions

The integration of photogrammetry (SfM) with LiDAR available in consumer mobile devices such as the iPhone enables quick and straightforward acquisition of data in the form of a point cloud, which can serve as a basis for generating a highly accurate Digital Elevation Model (DEM). However, it should be noted that while the data acquisition and uploading to the cloud proceed smoothly, the subsequent stages require significantly more effort and specialized knowledge.

The experiment using the iPhone 15 Pro yielded satisfactory results, despite the fact that the entire procedure required performing a series of steps. Some calculations were carried out in the cloud, which is important, as not everyone has access to a workstation capable of processing large volumes of data.

The use of LiDAR enabled the acquisition of depth files, which enhanced the quality of the collected data. Moreover, the geometric and spatial operations carried out resulted in a terrain model characterized by high spatial resolution, relatively low elevation differences, and low geolocation errors in relation to the base model. However, if the aim of the study is to achieve higher, namely geodetic, positional accuracy than that presented in this article, the iPhone should be equipped with a viDoc RTK antenna. Nevertheless, purchasing such a device involves incurring additional costs.

The advantages of the iPhone 15 Pro include its advanced camera system, the presence of a LiDAR sensor, compact size, and low weight, all of which encourage single-person surveying. The only requirement is the ability to correctly perform the scanning procedure.

Using an iPhone with a built-in LiDAR sensor is highly recommended and can be employed as a mobile scanning device for small objects, especially when the priority is to obtain a high-resolution point cloud and a Digital Elevation Model (DEM).

Acknowledgments

The author is grateful to the management of the Wawel Royal Castle for granting permission to conduct this experiment.

References

[1] Z. Wang, "Review of real-time three-dimensional shape measurement techniques," *Measurement*, vol. 156, Article Number: 107624, 2020. DOI: 10.1016/j.measurement.2020.107624.

[2] National Oceanic and Atmospheric Administration (NOAA) Coastal Services Center, *Lidar 101: An Introduction to Lidar Technology, Data, and Applications*. Revised. Charleston: SC: NOAA Coastal Services Center, 2012.

[3] J. L. Carrivick, M. W. Smith, and D. J. Quincey, *Structure from Motion in the Geosciences,* John Wiley & Sons Ltd, 2016.

[4] M. Dworzak, A. Biessikirski, J. Pyra, A. Sołtys, and J. Winzer, "Preliminary study of the digital non-metric terrestrial photogrammetry carried out by the use of the SfM method (Structure-from-Motion) applicability in blasting works," *Przegląd Górniczy*, vol. 71, no. 9, pp. 61–68, 2015.

[5] A. Saputra, T. Rahardianto, and C. Gomez, "The Application of Structure from Motion (SfM) to Identify the Geological Structure and Outcrop Studies," *AIP Conf. Proc.* 1857, Article Number: 030001, 2017. DOI: 10.1063/1.4987060.

[6] L. Javernick, J. Brasington, and B. Caruso, "Modeling the topography of shallow braided rivers using Structure-from-Motion photogrammetry," *Geomorphology*, vol. 213, pp. 166–182, 2014. DOI:10.1016/j.geomorph.2014.01.006.

[7] E. Grottoli, M. Biausque, D. Rogers, D. W. T. Jackson, and J. A. G. Cooper, "Structure-from-Motion-Derived Digital Surface Models from Historical Aerial Photographs: A New 3D Application for Coastal Dune Monitoring," *Remote Sens.*, vol. 13, no. 1, Article Number: 95, 2021. DOI: 10.3390/rs13010095.

[8] F. Brandolini and G. Patrucco, "Structure-from-Motion (SFM) Photogrammetry as a Non-Invasive Methodology to Digitalize Historical Documents: A Highly Flexible and Low-Cost Approach?," *Heritage*, vol. 2, no. 3, pp. 2124–2136, 2019. DOI: 10.3390/heritage2030128.

[9] N. Mölg and T. Bolch, "Structure-from-Motion Using Historical Aerial Images to Analyse Changes in Glacier Surface Elevation," *Remote Sens.*, vol. 9, no. 10, Article Number: 1021, 2017. DOI: 10.3390/rs9101021.

[10] J. Królikowski, M. Wywiał, and G. Durło, "Skaner spod strzechy," *Geodeta*, 7(326), pp. 40–44, 2022.

[11] S. Tatsumi, K. Yamaguchi, and N. Furuya, "ForestScanner: A mobile application for measuring and mapping trees with LiDAR-equipped iPhone and iPad," *Methods Ecol. Evol.*, vol. 14, no. 7, pp. 1603–1609, 2023. DOI: 10.1111/2041-210X.13900.

[12] S. Kottner, M. J. Thali, and D. Gascho, "Using the iPhone's LiDAR technology to capture 3D forensic data at crime and crash scenes," *Forensic Imaging*, vol. 32, Article Number: 200535, 2023. DOI: 10.1016/j.fri.2023.200535.

[13] P. P. C. Chase, K. H. Clarke, A. J. Hawkes, S. Jabari, and J. S. Jakus, "Apple iPhone 13 Pro LiDAR accuracy assessment for engineering applications," in *Transforming Construction with Reality Capture Technologies: The Digital Reality of Tomorrow*, August 23-25, 2022, Fredericton, New Brunswick, Canada, pp. 1–10, 2022.

[14] W. Rutkowski and T. Lipecki, "Use of the iPhone 13 Pro LiDAR Scanner for Inspection and Measurement in the Mineshaft Sinking Process," *Remote Sens.*, vol. 15, no. 21, Article Number: 5089, 2023. DOI:10.3390/rs15215089.

[15] W. Błaszczak-Bąk, C. Suchocki, T. Kozakiewicz, and J. Janicka, "Measurement methodology for surface defects inventory of building wall using smartphone with light detection and ranging sensor," *Measurement*, vol. 219, Article Number: 113286, 2023. DOI:10.1016/j.measurement.2023.113286.
[16] C. Askar and H. Sternberg, "Use of Smartphone Lidar Technology for Low-Cost 3D Building Documentation with iPhone 13 Pro: A Comparative Analysis of Mobile Scanning Applications," *Geomatics*, vol. 3, no. 4, pp. 563–579, 2023. DOI: 10.3390/geomatics3040030.
[17] T. Mikita, D. Krausková, P. Hrůza, M. Cibulka, and Z. Patočka, "Forest Road Wearing Course Damage Assessment Possibilities with Different Types of Laser Scanning Methods including New iPhone LiDAR Scanning Apps," *Forests*, vol. 13, no. 11, Article Number: 1763, 2022. DOI: 10.3390/f13111763.
[18] E. B. Dörtbudak and Ş. Akça, "Investigating the utilization of iPhone lidar sensor in documenting cultural heritage," in *7th Intercontinental Geoinformation Days (IGD*) – 18-19 November 2023 – Peshawar, Pakistan, vol. 7, pp. 217–221, 2023.
[19] G. Luetzenburg, A. Kroon, and A. A. Bjørk, "Evaluation of the Apple iPhone 12 Pro LiDAR for an Application in Geosciences," *Sci. Rep*., vol. 11, no. 1, Article Number: 22221, 2021. DOI: 10.1038/s41598-021-01763-9.
[20] "Hillshade - WMTS," https://www.geoportal.gov.pl/ [accessed on 16.09.2024].
[21] "Standard Orthophotomap - WMTS," https://www.geoportal.gov.pl/ [accessed on 16.09.2024].
[22] "Sprawozdania z badań archeologicznych wykonanych przez dział archeologii PZS i KOZK na Wawelu w 1964 roku (AZK PZS 612/36)," 1964.
[23] "iPhone 15 Pro - Tech Specs," https://support.apple.com/en-us/111829 [accessed on 25.07.2025].
[24] "Sony ISP from IMX591, 10.1µm Pixel Pitch, 0.01MP, Stacked Back-Illuminated Direct-Time of Flight (d-ToF) SPAD Sensor Advanced Floorplan Analysis.," https://www.techinsights.com/blog/sony-isp-imx591-101mm-pixel-pitch-001mp-stacked-back-illuminated-direct-time-flight-d-tof-spad?utm_source=direct&utm_medium=website [accessed on 25.07.2025].
[25] "National Integration of Topographic Object Databases (KIBDOT) - WMS," https://www.geoportal.gov.pl/ [accessed on 19.08.2024].
[26] J. Zawadzki, *Metody geostatystyczne dla kierunków przyrodniczych i technicznych*, Warszawa: Oficyna Wydawnicza Politechniki Warszawskiej, 2011.
[27] R. Zarychta and A. Zarychta, "Application of geostatistical approach in generating DEM for relief studies using UAV in forest areas," *Geomorphology*, vol. 487. Article Number: 109916, 2025. DOI: 10.1016/j.geomorph.2025.109916.
[28] D. Lorek, "Ocena doboru metod implementacji XIX-wiecznych map topograficznych do współczesnego układu współrzędnych w aplikacji QGIS," *Badania Fizjogr.,* Seria A - Geografia Fizyczna, vol. 68, pp. 47–59, 2017. DOI: 10.14746/bfg.2017.8.4.
[29] R. Zarychta, A. Zarychta, and K. Bzdęga, "Ecogeomorphological Transformations of Aeolian Form—The Case of a Parabolic Dune, Poland," *Remote Sens*., vol. 13, no. 19, Article Number: 3937, 2021. DOI: 10.3390/rs13193937.
[30] "Model quasi-geoidy PL-geoid2021 modelem obowiązującym" GUGiK, 2022. https://www.gov.pl/web/gugik/model-quasi-geoidy-pl-geoid2021-modelem-obowiazujacym [accessed on 25.07.2025].

Received: October 22, 2025
Accepted: August 08, 2026